Climate-dependent malaria disease transmission model and its analysis

Kassahun Workalemahu Gashaw

Department of Mathematics, Addis Ababa University
P.O.Box 1176, Addis Ababa, Ethiopia
kassahun.workalemahu@aau.edu.et

Semu Mitiku Kassa[1,2]

(1) Department of Mathematics and Statistical Sciences, Botswana International University of Science and Technology (BIUST)
P/Bag 16, Palapye, Botswana
kassas@biust.ac.bw
(2) Department of Mathematics, Addis Ababa University
P.O.Box 1176, Addis Ababa, Ethiopia

Rachid Ouifki

Department of Mathematics and Applied Mathematics, University of Pretoria
South Africa
Rachid.Ouifki@up.ac.za

Abstract. Malaria infection continues to be a major problem in many parts of the world including Africa. Environmental variables are known to affect significantly the population dynamics and abundance of insects, major catalysts of vector-borne diseases, but the exact extent and consequences of this sensitivity are not yet well-established. To assess the impact of the variability in temperature and rainfall on the transmission dynamics of malaria in a population, we propose a model consisting of system of non-autonomous deterministic equations that incorporate the effect of both temperature and rainfall to the dispersion and mortality rate of adult mosquitoes. The model has been validated using epidemiological data collected from western region of Ethiopia, by considering the trends for cases of malaria and the climate variation in the region. Further, a mathematical analysis is performed to assess the impact of temperature and rainfall change on the transmission dynamics of the model. The periodic variation of seasonal variables as well as the non-periodic variation due to the long term climate variation have been incorporated and analyzed. In both periodic and non-periodic cases, it has been shown that the disease-free solution of the model is globally asymptotically stable when the basic reproduction ratio is less than unity in the periodic system and when the threshold function is less than unity in the non-periodic system. The disease is uniformly persistent when the basic reproduction ratio is greater than unity in the periodic system and when the threshold function is greater than unity in the non-periodic

system.

Keywords: Climate dependent malaria model; Asymptotic stability; Periodic and non-periodic climate dependent growth rates; validation using epidemiological data.

1. Introduction

Malaria is caused by a parasite called *Plasmodium falciparum* and is transmitted by *Anopheles* mosquitoes. The vector that spreads malaria is sensitive to climate variables, especially rainfall and temperature [11,21,32]. Although non-climatic factors such as epidemiological, environmental, socio-economic and demographic factors are known to influence the dynamics of malaria and other vector-borne diseases, changes in temperature and rainfall have their own influences (see [23] and some of the references therein).

Despite its strong connection with malaria, climate may not be the only cause for future malaria transmission rates worldwide mainly because there are many other factors that affect the spread of the disease including socioeconomic development, drug resistance, and immunity [17].

Climate factors such as temperature, humidity, rainfall and wind significantly affect the vector's life-cycle and, consequently, the abundance of mosquitoes in populations. Malaria-climate connection in the East African highlands was identified in the 1980s when there was a series of malaria epidemics connected to increases and anomalies in mean monthly maximum temperatures and increase in rainfall in the highlands [12,31,27,24]. According to the International Panel on Climate Change (IPCC) Fourth Assessment Report, climate change has already altered the distribution of some disease vectors. In East Africa, climate scenarios suggest longer malaria transmission seasons and geographic expansion of the disease into highland areas. The frequency and size of epidemics increased with serious outbreaks in 1995, 1998 and 2002, corresponding to climate variations such as a significant increase ($\geq 3^{\circ}$C) in mean temperatures, high rainfall, drought and El Nino events (see [25], and the references therein). Some studies have shown that an increase in temperature has allowed the introduction of malaria into higher altitude areas in Colombia, Ethiopia and Kenya, where it was previously too cold for the disease to thrive [34]. This has put millions of people at risk for the disease. While we know that climate can affect malaria transmission, the impact of climate change on regional and global malaria cases and deaths is even less understood.

Several mathematical models have been designed to assess the impact of climate change and seasonality on the transmission dynamics of malaria (see [1] and the references therein). Parham et al. [29] have developed a mathematical model to investigate the impact of environmental factors (temperature and rainfall) in the transmission dynamics by defining the adult mosquito birth rate as a function of temperature and rainfall while other parameters are dependent only on either temperature or rainfall alone. They validated also their results by considering the mosquito population in Tanzania where malaria is highly-endemic, expressing the

temperature and rainfall by single cosine function which may ignore the actual variations in the environmental factors and has to be extended and consolidated by setting up a model that incorporates the effects of both temperature and rainfall in the birth and death rates of the vector population. Specially a climate driven model with parameters dependent on both climate variables (temperature and rainfall) in a non-periodic environment is not yet developed as far as the knowledge of the authors go and this work gives much emphasis on this issue.
Agusto et al. [2] developed temperature-dependent deterministic model to gain qualitative insight into the effects of temperature variability only on malaria transmission dynamics. The authors incorporated a gradual increase in infection-acquired immunity via repeated exposure to malaria infection. The focus of their study was on analyzing the impact of changing temperature and temperature variability on short-term malaria dynamics (due, for instance, to seasonality), and not on long-term malaria dynamics (due to climate change).
Motivated by the works of [19],[16],[38], Wang et al. [36] proposed a malaria transmission non-autonomous model with periodic environment without incorporating the climate factors in their model. Wang et al. computed a basic reproduction number and have shown that the disease-free periodic solution of their model is globally asymptotically stable when the basic reproduction number is less than unity, while the disease is uniformly persistent and there is at least one positive periodic solution when the basic reproduction number is greater than unity. That is, they have shown that the basic reproduction number is the threshold value determining the extinction and the uniform persistence of the disease.
Okuneye and Gumel [23] extended the work in [30] by designing a new temperature and rainfall-dependent mechanistic malaria model that incorporates some more pertinent climatic and non-climatic features and factors not considered in [30] (such as host age-structure, dynamics of immature mosquitoes, reduced susceptibility due to prior malaria infection etc.) and analyzed the full non-autonomous model but periodic and carried out uncertainty and sensitivity analyses on the parameters of the model with the mortality rate of juvenile and adult mosquitoes dependent only on temperature.

The purpose of this study is to investigate a climate driven malaria disease transmission model incorporating the effect of temperature in the biting rate and the effects of both temperature and rainfall in the birth rate and death rate of the vector population in both periodic and non-periodic environments by using the standard model considering the dynamics of the adult mosquito population only and referring the works [29,23]. The study assesses the potential change in malaria risk caused by seasonal variations in temperature and rainfall which is important to investigate the dynamics of the disease in a short term basis. Moreover, as climate impact upon the distribution of the malaria transmission in space and time is not always periodic, we need to investigate the potential change in malaria risk caused by the variations in temperature and rainfall in the non-periodic case as well. Exploring

the dynamics of the disease in a long term basis and the information provided here might serve as an important contribution for strategic planning of malaria control in a long period of time in the future.

This paper is organized as follows, in Section 2 we formulated a model consisting of ordinary differential equations (ODE) that describe the interactions between humans and mosquitoes populations and the underlying assumptions. In Section 3, a positively invariant set with respect to the system will be identified and shown to be a global attractor of all positive solutions of the system to confirm the biological well posedness of the model system. In Sections 4, the non-autonomous periodic system is reviewed while the non-autonomous non-periodic system is discussed and analysed in Section 5 and we show the simulation results to illustrate the population dynamics in both environments at the end of the latter sections. Our conclusions are discussed in Section 6.

2. Model Formulation

Following the works in [29,23], where the authors developed a framework for understanding the impact of climate on malaria dynamics, we use the standard deterministic malaria disease transmission model with an SIR structure for humans and an SI structure for mosquitoes. Climate change is known to affect several parameters in the epidemiology of malaria and hence predicting climate change effects on disease transmission requires a framework that specifically incorporates the role of each climate sensitive parameter. Some models examining the contribution of climate change have been explored [4,9,13,18,28].
The total human population (N_h) is divided into three classes: susceptible (S_h), infectious (I_h) and recovered (R_h). People enter the susceptible class either through birth (at a constant per capita rate) or through immigration (at a constant rate) or after recovering from the disease. When an infectious mosquito bites a susceptible human, there is some non-zero probability that the parasite (in the form of sporozoites) will be passed on to the human.
The rate of infection of a susceptible individual is dependent on the mosquito biting rate ϕ (daily feeding rate of a vector on a host) defined using the exponential function of the temperature variable, T (Fig. 1) as

$$\begin{aligned}\phi(T) =& 0.48\exp(0.14(T-23))/(\exp(-0.14(T-23))+\exp(0.14(T-23)))\\ &+(-0.48\exp(0.32(T-37))/(\exp(-0.32(T-37))+\exp(0.32(T-37)))\end{aligned} \tag{2.1}$$

with standard incidence rate of $\frac{\beta_{vh}\phi I_v S_h}{N_h}$, where β_{vh} is the probability that the bites by an infectious mosquitoes on susceptible humans produce infection.
Infected humans recover at a constant rate r_h for some period of time and move to the recovered class R_h. The recovered humans may develop some immunity to the disease and do not get clinically ill, but they may still harbor low levels of parasite in their blood streams. However, since the rate of infections from this group of indi-

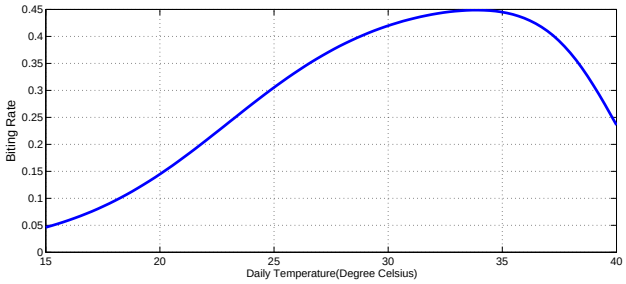

Fig. 1: The mosquito biting rate (daily feeding rate of a vector on a host) $\phi(T)$.

viduals is assumed to be very small, we omitted its impact in our model. After some period of time, recovered humans loose their immunity and return to the susceptible class at a constant rate σ. Infected individuals who do not get treatment may die from infection at a constant rate μ_d. Humans die naturally at a non-malaria related per capita natural mortality constant rate μ_h.

As only female mosquitoes take blood-meals, the model considers only the female mosquito population. Instead of detailing the dynamics of all aquatic stages, we rather used an emergence rate $\Lambda_v(T, R)$ of adult female anopheles mosquitoes which is assumed to be a function of rainfall R and temperature T that recasts all the historical dynamics from egg hatching to emergence.
The functions $T = T(t)$ and $R = R(t)$ denote the temperature and the rainfall quantity at time t respectively.
It is often difficult to establish significant and stationary relationships between the amount of precipitation and mosquito abundance or malaria disease transmission patterns. Rainfall can alter the abundance and type of aquatic habitats available to the mosquito for the deposition of eggs (oviposition) and the subsequent development of the immature stages [33]. We assume that at any time t, the time variation of the emergence rate of adult female anopheles mosquitoes $\Lambda_v(T, R)$ is defined by Equation (2) in [29],(Fig. 2):

$$\Lambda_v(T, R) = \frac{3.375(4R(50 - R))^3 \exp(-0.00554T + 0.06737)}{50^6(2 + (0.00554T - 0.06737)^{-1})} \tag{2.2}$$

The adult female anopheles mosquitoes population is subdivided into two classes: susceptible (S_v) and infectious (I_v). Susceptible adult mosquitoes are recruited at a rate $\Lambda_v(T, R)$. The rate of infection for a susceptible mosquito depends on the mosquito's biting rate in which the transmission rate from infectious host to susceptible vector is given by $\frac{\beta_{hv}\phi I_h S_v}{N_h}$ where β_{hv} represents the probability that a susceptible mosquito get infected when biting an infected human. Although the rainfall effect on the survival of adult mosquitoes is not significantly high, its influence can not be ignored as the increased near-surface humidity associated with rainfall

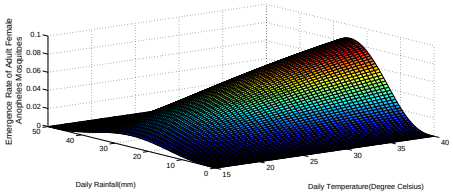

Fig. 2: Emergence rate of adult female anopheles mosquitoes $\Lambda_v(T, R)$.

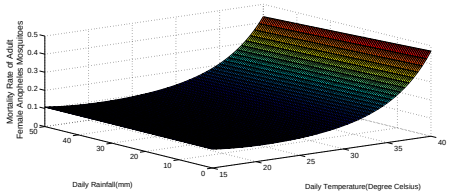

Fig. 3: Mortality rate of adult female anopheles mosquitoes $\mu_v(T, R)$.

enhances mosquito flight activity and host-seeking behavior [33]. Mosquitoes leave the population through a per capita climate-dependent(temperature and rainfall) natural death rate given by (Fig.3):

$$\mu_v(T, R) = 0.0886 \exp\left(\left(\frac{-0.01R + 1.01T - 21.211}{14.852}\right)^2\right) \tag{2.3}$$

which is assumed to follow an exponential distribution in temperature and rainfall [5].

The transmission interactions between hosts and vectors can be described by the following system of non-autonomous differential equations where some coefficients or parameters depend on time through time-dependent temperature and/or rainfall:

$$\begin{aligned}
\frac{dS_v}{dt} &= \Lambda_v(T, R) - \lambda_v(T)S_v - \mu_v(T, R)S_v, \\
\frac{dI_v}{dt} &= \lambda_v(T)S_v - \mu_v(T, R)I_v, \\
\frac{dS_h}{dt} &= \Lambda_h - \lambda_h(T)S_h + \sigma R_h - \mu_h S_h, \qquad . \\
\frac{dI_h}{dt} &= \lambda_h(T)S_h - (\mu_h + r_h + \mu_d)I_h, \\
\frac{dR_h}{dt} &= r_h I_h - (\mu_h + \sigma)R_h,
\end{aligned} \tag{2.4}$$

where $\lambda_h(T) = \frac{\beta_{vh}\phi(T)I_v}{N_h}$ and $\lambda_v(T) = \frac{\beta_{hv}\phi(T)I_h}{N_h}$ represent the force of infection of humans and mosquitoes, respectively.

$$N_h = S_h + I_h + R_h, \tag{2.5}$$

$$N_v = S_v + I_v \tag{2.6}$$

are the total human and mosquito population, respectively.

To simplify the mathematical analysis of the model in the coming sections, we didn't consider the different aquatic stages of the vector population. A similar model for periodic case with aquatic stages is considered in [23].

Table 1: Description of variables and parameters of the model.

Symbol	Description
$\phi(T)$	The biting rate function of mosquitoes
β_{vh}	Probability of human getting infected per enough contact with infected mosquito
β_{hv}	Probability of mosquito getting infected per each enough contact with infected human
Λ_h	Recruitment rate of susceptible humans
μ_h	*Per capita* natural death rate for humans
r_h	human recovery rate
$\Lambda_v(T,R)$	Emergence rate function of female mosquitoes
σ	*Per capita* rate of loss of immunity for human
μ_d	*Per capita* disease induced death rate for human
$\mu_v(T,R)$	Mosquito per capita death rate function

In view of the biological background of system (2.4), in this study we only consider the solution of system (2.4) starting at $t = 0$ with initial values:

$$S_v(0) \geq 0, \quad I_v(0) \geq 0, \quad S_h(0) \geq 0, \quad I_h(0) \geq 0 \quad \text{and} \quad R_h(0) \geq 0. \tag{2.7}$$

For the purpose of our mathematical analyses, we note that the climate-dependent functions satisfy the following assumptions:

- (H_1) $\Lambda_v(T,R)$, $\mu_v(T,R)$, $\lambda_h(T)$ and $\lambda_v(T)$ are continuous functions in T and R.
- (H_2) $\Lambda_v(T,R) > 0$, $\mu_v(T,R) > 0$, $\lambda_h(T) \geq 0$ and $\lambda_v(T) \geq 0$ with $\lambda_h(T) \not\equiv 0$ and $\lambda_v(T) \not\equiv$ for all T and R.

These assumptions guarantee the existence and continuity of solutions and ensures that the force of infection is active, not identically zero.

When $I_h(t) \equiv 0, R_h(t) \equiv 0$ and $I_v(t) \equiv 0$, we obtain the following two subsystem of system (2.4)

$$\dot{S}_h(t) = \Lambda_h - \mu_h S_h(t), \tag{2.8}$$

$$\dot{S}_v(t) = \Lambda_v(T(t), R(t)) - \mu_v(T(t), R(t)) S_v(t). \tag{2.9}$$

We see that system (2.4) has a disease-free solution (DFS)

$$E_0^*(t) = (S_v^*(t), 0, \frac{\Lambda_h}{\mu_h}, 0, 0), \tag{2.10}$$

where

$$S_v^*(t) = e^{-\int_0^t \mu_v(T(\tau),R(\tau))d\tau} \left\{ S_v(0) + \int_0^t \Lambda_v(T(s), R(s)) e^{\int_0^s \mu_v(T(\sigma),R(\sigma))d\sigma} ds \right\}$$

is the solution of (2.9).

3. Model analysis

Before we proceed with the mathematical analysis, we need to show that the model is well posed in a biologically feasible domain.

3.1. *Model well-posedness*

We analyze (2.4) in a biologically-feasible region for both human and mosquito populations.
Let $m_v := \inf\{\mu_v(T(\tau), R(\tau)), \tau \geq 0\}$ and $M_v := \sup\{\Lambda_v(T(s), R(s)), s \geq 0\}$,

we have the following result:

Proposition 3.1. *If the initial conditions $S_v(0), I_v(0), S_h(0), I_h(0)$ and $R_h(0)$ are non-negative then the corresponding solution $(S_v(t), I_v(t), S_h(t), I_h(t), R_h(t))$ of the malaria model (2.4) is non-negative for all $t > 0$.*
Moreover,

$$\limsup_{t\to\infty} N_h(t) \leq \frac{\Lambda_h}{\mu_h} \text{ and } \limsup_{t\to\infty} N_v(t) \leq \frac{M_v}{m_v}.$$

Furthermore, we have the following invariance properties:

i. if $N_h(0) \leq \frac{\Lambda_h}{\mu_h}$ then $N_h(t) \leq \frac{\Lambda_h}{\mu_h}$
ii. if $N_v(0) \leq \frac{M_v}{m_v}$ then $N_v(t) \leq \frac{M_v}{m_v}$.

In particular, the regions $\mathbb{R}^2_+ \times \mathcal{D}_h$ and $\mathcal{D}_v \times \mathbb{R}^3_+$ with

$$\mathcal{D}_h = \left\{(S_h, I_h, R_h) \in \mathbb{R}^3_+ : S_h + I_h + R_h \leq \frac{\Lambda_h}{\mu_h}\right\}$$
$$\text{and} \quad \mathcal{D}_V = \left\{(S_v, I_v) \in \mathbb{R}^2_+ : S_v + I_v \leq \frac{M_v}{m_v}\right\}$$

are positively-invariant.

The proof of this proposition can be found in the appendix.
In the view of Proposition 3.1 above, we conclude that system (2.4) is epidemiologically feasible and mathematically well-posed in $\mathcal{D} = \mathcal{D}_h \times \mathcal{D}_v$.

3.2. *Periodic System*

In this section, we assume that variations in temperature and rainfall are seasonal causing the corresponding temperature and/or rainfall dependent parameters in the malaria model to vary in seasonal manner. Assessment of the potential change in malaria risk caused by seasonal variations in temperature and rainfall is important to investigate the dynamics of the disease in a short term basis. The information provided here might serve as an important contribution for strategic planning of

malaria control in a short period of time in the future.

For shorter period of study time the climatic values change seasonally and hence they are very much periodic in time. By considering periodicity in the climate variables and the corresponding parameters dependent on the periodic climate variables (temperature and rainfall), we analyze model (2.4) in the periodic environment. Thus the system will have time dependent periodic coefficients as climate variables could be expressed as a function of time.

3.3. *Some Results of the Model in the Periodic Environment*

Using the initial data (2.7) and restricting the assumptions (H_1) and (H_2) to the periodic environment we have the following assumptions:

- (H_1') $\Lambda_v(T(t),R(t))$, $\mu_v(T(t),R(t))$, $\lambda_h(T(t))$ and $\lambda_v(T(t))$ are continuous and ω-periodic functions.
- (H_2') $\int_0^\omega \Lambda_v(T(t),R(t))dt > 0$.

For convenience, we change the notation of $\Lambda_v\left(T\left(t\right),R\left(t\right)\right)$, $\mu_v\left(T\left(t\right),R\left(t\right)\right)$ and $\lambda_v\left(T\left(t\right)\right)$, to $\Lambda_v\left(t\right)$, $\mu_v\left(t\right)$ and $\lambda_v\left(t\right)$ respectively.

Lemma 3.2. *If (H_1') and (H_2') hold, the function*

$$S_v^*\left(t\right) = S_v^0 e^{-\int_0^t \mu_v(\tau)d\tau} + \int_0^t \Lambda_v\left(s\right) e^{-\int_s^t \mu_v(\tau)d\tau} ds$$

where $S_v^0 = \left(\int_0^\omega \Lambda_v\left(s\right) e^{-\int_s^\omega \mu_v(\tau)d\tau} ds\right) \Big/ \left(1 - e^{-\int_0^\omega \mu_v(\tau)d\tau}\right)$ *is an ω-periodic disease free solution of equation* (2.9).

Proof. Using the variation of constants formula, we show that for any $t, \tau \geq 0$ the solution of equation (2.9) satisfies

$$S_v\left(t\right) = S_v\left(\tau\right) e^{-\int_\tau^t \mu_v(\tau)d\tau} + \int_\tau^t \Lambda_v\left(s\right) e^{-\int_s^t \mu_v(\tau)d\tau} ds. \tag{3.1}$$

In particular, we have

$$S_v\left(t+\omega\right) = S_v\left(\omega\right) e^{-\int_\omega^{t+\omega} \mu_v(\tau)d\tau} + \int_\omega^{t+\omega} \Lambda_v\left(s\right) e^{-\int_s^{t+\omega} \mu_v(\tau)d\tau} ds. \tag{3.2}$$

Since μ_v is ω-periodic, then $e^{-\int_\omega^{t+\omega} \mu_v(\tau)d\tau} = e^{-\int_\omega^{t+\omega} \mu_v(\tau-\omega)d\tau}$, which by using the change of variable $s = \tau - \omega$, leads to

$$e^{-\int_\omega^{t+\omega} \mu_v(\tau-\omega)d\tau} = e^{-\int_0^t \mu_v(s)ds}. \tag{3.3}$$

Similarly, since Λ_v is also assumed to be ω-periodic, we have

$$\begin{aligned}\int_\omega^{t+\omega} \Lambda_v\left(\tau\right) e^{-\int_\tau^{t+\omega} \mu_v(s)ds} d\tau &= \int_\omega^{t+\omega} \Lambda_v\left(\tau-\omega\right) e^{-\int_{\tau-\omega+\omega}^{t+\omega} \mu_v(s)ds} d\tau \\ &= \int_\omega^{t+\omega} \Lambda_v\left(\tau-\omega\right) e^{-\int_{\tau-\omega}^{t} \mu_v(s)ds} d\tau \text{ (because } \mu_v \text{ is}\omega\text{-periodic).}\end{aligned}$$

Letting $x=\tau-\omega$, gives $\int_{\omega}^{t+\omega}\Lambda_v(\tau-\omega)\,e^{-\int_{\tau-\omega}^{t}\mu_v(s)ds}d\tau=\int_0^t\Lambda_v(x)\,e^{-\int_x^t\mu_v(s)ds}dx$ which implies that

$$\int_{\omega}^{t+\omega}\Lambda_v(\tau)\,e^{-\int_{\tau}^{t+\omega}\mu_v(s)ds}d\tau=\int_0^t\Lambda_v(x)\,e^{-\int_x^t\mu_v(s)ds}dx. \tag{3.4}$$

Furthermore, substituting (3.3) and (3.4) in (3.2), we obtain

$$S_v(t+\omega)=S_v(\omega)\,e^{-\int_0^t\mu_v(s)ds}+\int_0^t\Lambda_v(x)\,e^{-\int_x^t\mu_v(s)ds}dx.$$

On the other hand, we have from (3.1) that

$$S_v(\omega)=S_v(0)\,e^{-\int_0^{\omega}\mu_v(\tau)d\tau}+\int_0^{\omega}\Lambda_v(s)\,e^{-\int_s^{\omega}\mu_v(\tau)d\tau}ds.$$

Since $S_v(0)=\left(\int_0^{\omega}\Lambda_v(s)\,e^{-\int_s^{\omega}\mu_v(\tau)d\tau}ds\right)\Big/\left(1-e^{-\int_0^{\omega}\mu_v(\tau)d\tau}\right)$, then $S_v(\omega)=S_v(0)$. Thus

$$S_v(t+\omega)=S_v(0)\,e^{-\int_0^t\mu_v(s)ds}+\int_0^t\Lambda_v(x)\,e^{-\int_x^t\mu_v(s)ds}dx=S_v(t).$$

□

Now following [36], based on the assumptions H_1 and H_2, we can compute the basic reproduction ratio of system (2.4) using the way it is given in ([35],[37]).

Let

$$\mathcal{F}(t,x)=\begin{pmatrix}\lambda_v(t)S_v\\ \lambda_h(t)S_h\\ 0\\ 0\\ 0\end{pmatrix},\quad \mathcal{V}^-(t,x)=\begin{pmatrix}\mu_v(T(t),R(t))I_v\\ (\mu_h+r_h+\mu_d)I_h\\ \lambda_v(t)S_v+\mu_v(T(t),R(t))S_v\\ \lambda_h(t)S_h+\mu_hS_h\\ \mu_hR_h+\sigma R_h\end{pmatrix}$$

$$\text{and}\quad \mathcal{V}^+(t,x)=\begin{pmatrix}0\\ 0\\ \Lambda_v(T(t),R(t))\\ \Lambda_h+\sigma R_h\\ r_hI_h\end{pmatrix}$$

where $x=(S_v,I_v,S_h,I_h,R_h)^T$, then system (2.4) equals to the following form

$$\dot{x}(t)=\mathcal{F}(t,x)-\mathcal{V}(t,x)\triangleq f(t,x(t)), \tag{3.5}$$

where $\mathcal{V}(t,x)=\mathcal{V}^-(t,x)-\mathcal{V}^+(t,x)$.
It can be verified that system (2.4) satisfies assumptions (A1)-(A7) in [37].
Let

$$F(t)=\left(\frac{\partial\mathcal{F}_i(t,E_0^*(t))}{\partial x_j}\right)_{1\le i,j,\le m},\quad V(t)=\left(\frac{\partial\mathcal{V}_i(t,E_0^*(t))}{\partial x_j}\right)_{1\le i,j,\le m}, \tag{3.6}$$

In view of the periodic environment, we suppose that $\varphi(s)$ is the initial distribution of infectious individuals, which is assumed to be ω-periodic in s. Then $F(s)\varphi(s)$ is the total distribution of new infections produced by the infected individuals who were introduced at time s. Let $Y(t,s)$ denote the matrix solution of the initial value problem $\frac{d}{dt}Y(t,s) = -V(t)Y(t,s), Y(s,s) = I$ where I denotes the identity matrix. Then, for any $t \geq s$, $Y(t,s)F(s)\phi(s)$ represents the distribution of those infected individuals who were newly infected at time s and remain in the infected compartments at time t. It follows that

$$\psi(t) := \int_{-\infty}^{0} Y(t,s)F(s)\varphi(s)ds = \int_{0}^{\infty} Y(t,t-a)F(t-a)\varphi(t-a)da$$

is the distribution of cumulative new infections at time t produced by all those infected individuals $\varphi(s)$ introduced at previous time to t.
Let C_ω be the ordered Banach space of all ω-periodic functions from $\mathbb{R} \to \mathbb{R}^m$, which is equipped with the maximum norm $||.||$ and the positive cone

$$C_\omega^+ := \{\varphi \in C_\omega : \varphi(t)) \geq 0 \text{ for all } t \in \mathbb{R}\}.$$

Then we can define a linear operator $L : C_\omega \to C_\omega$ by

$$(L\varphi)(t) = \int_{0}^{\infty} Y(t,t-a)F(t-a)\varphi(t-a)da \text{ for all } t \in \mathbb{R}, \quad \varphi \in C_\omega. \tag{3.7}$$

Motivated by the concept of next generation matrices introduced in ([10], [35]), we call L the next infection operator, and define the spectral radius of L as the basic reproduction ratio

$$\mathcal{R}_0 := \rho(L) \tag{3.8}$$

for the periodic epidemic model (3.5).

Lemma 3.3. *(Lemma 4 in [36]) Assume that (A1)-(A7) in [37] hold. Then the following statements are valid:*

(i) $\mathcal{R}_0 = 1$ *if and only if* $\rho(\Phi_{F-V}(\omega)) = 1$*;*
(ii) $\mathcal{R}_0 > 1$ *if and only if* $\rho(\Phi_{F-V}(\omega)) > 1$*;*
(iii) $\mathcal{R}_0 < 1$ *if and only if* $\rho(\Phi_{F-V}(\omega)) < 1$*.*

where

$$F(t) = \begin{pmatrix} 0 & \frac{\beta_{hv}\phi(T(t))}{N_h(t)}S_v^*(t) \\ \frac{\beta_{vh}\phi(T(t))\Lambda_h}{N_h(t)\mu_h} & 0 \end{pmatrix}, \quad V(t) = \begin{pmatrix} \mu_v(T(t),R(t)) & 0 \\ 0 & \mu_h + r_h + \mu_d \end{pmatrix}$$

Thus, the disease-free periodic solution (2.10) *is asymptotically stable if* $\mathcal{R}_0 < 1$*, and unstable if* $\mathcal{R}_0 > 1$*.*

Theorem 3.4. *If* $\mathcal{R}_0 < 1$*, then the disease-free periodic solution* $E_0^*(t)$ *of system* (2.4) *is globally asymptotically stable.*

Theorem 3.5. *If $\mathcal{R}_0 > 1$, then system (2.4) is uniformly persistent. That is, there exists a positive constant ε, such that any solution $(S_v(t), I_v(t), S_h(t), I_h(t), R_h(t))$ of system (2.4) with initial conditions $S_v(0) \geq 0, I_v(0) \geq 0, S_h(0) \geq 0, I_h(0) \geq 0$ and $R_h(0) \geq 0$ satisfies*

$$\liminf_{t\to\infty}(S_v(t), I_v(t), S_h(t), I_h(t), R_h(t)) \geq (\varepsilon, \varepsilon, \varepsilon, \varepsilon, \varepsilon).$$

For the periodic system (2.4), a stability analysis similar to the works of [36] can be done using the basic reproduction ratio that satisfies the equivalence mentioned in Lemma 3.3. It can also be shown that the disease-free periodic solution (3.3) is globally asymptotically stable if $\mathcal{R}_0 < 1$ and the system (2.4) is uniformly persistent when $\mathcal{R}_0 > 1$ in a way exactly similar to the proofs given in [36].

3.4. *Autonomous version of the model*

In this section, we study the system with constant temperature and rainfall.

3.4.1. *The basic reproductive number*

To derive the basic reproductive number of the autonomous version of model (2.4), we use the method of next generation matrix formulated by Diekmann et al. [10] and van den Driessche and Watmough [35].
The rates of appearance of new infections and those representing the other transfers of individuals are respectively given by the following vectors:

$$\mathcal{F}(x) = \begin{pmatrix} \lambda_v S_v \\ \lambda_h S_h \\ 0 \\ 0 \\ 0 \end{pmatrix}, \mathcal{V}(x) = \begin{pmatrix} \mu_v I_v \\ (\mu_h + r_h + \mu_d) I_h \\ -\Lambda_v + \lambda_v S_v + \mu_v S_v \\ -\Lambda_h + \sigma R_h + \lambda_h S_h + \mu_h S_h \\ -r_h I_h + \mu_h R_h + \sigma R_h \end{pmatrix}. \tag{3.9}$$

The next generation matrix is given by FV^{-1}, where F (resp. V) is the jacobian matrix of $\mathcal{F}$ (resp. $\mathcal{V}$) at the disease free equilibrium

$$E_0^* = \left(\frac{\Lambda_v}{\mu_v}, 0, \frac{\Lambda_h}{\mu_h}, 0, 0\right).$$

We obtain

$$F = \begin{pmatrix} 0 & \frac{\beta_{hv}\phi\Lambda_v\mu_h}{\Lambda_h\mu_v} \\ \beta_{vh}\phi & 0 \end{pmatrix}, V = \begin{pmatrix} \mu_v & 0 \\ 0 & \mu_h + r_h + \mu_d \end{pmatrix}. \tag{3.10}$$

The basic reproductive number of model (2.4) is given by the spectral radius of the next generation matrix $\rho(FV^{-1})$,

$$\bar{\mathcal{R}}_0 = \sqrt{\frac{\beta_{vh}\beta_{hv}\phi^2\Lambda_v\mu_h}{\mu_v^2\Lambda_h\left(\mu_h + r_h + \mu_d\right)}} \tag{3.11}$$

3.4.2. *Sensitivity analysis of the basic reproductive number*

We will now analyze the sensitivity index of the basic reproductive number with respect to temperature and rainfall using the forward sensitivity index.

Definition 3.1. *The sensitivity index of a variable Y with respect to a parameter p is given by*

$$\Gamma_Y^p = \frac{\partial \Gamma}{\partial p}\frac{p}{Y}.$$

Using the definition above we calculate the sensitivity index of $\bar{\mathcal{R}}_0$ with respect to T and R using the expression of $\bar{\mathcal{R}}_0$, expressions (2.1), (2.2) and (2.3) and parameter values presented in Table (2). The results are plotted in Figures 4 and 5.

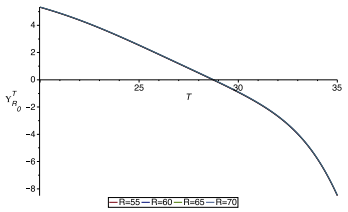

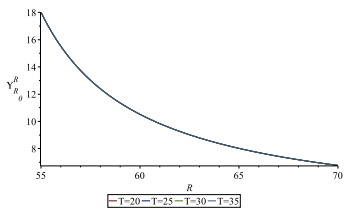

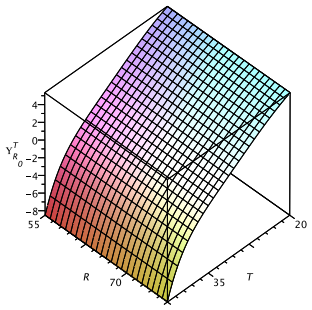

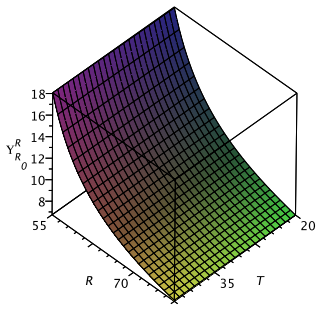

Fig. 4: Sensitivity index of $\bar{\mathcal{R}}_0$ with respect to temperature.

Fig. 5: Sensitivity index of $\bar{\mathcal{R}}_0$ with respect to rainfall.

We observe from these figures that the sensitivity index of $\bar{\mathcal{R}}_0$ with respect to rainfall seems to be independent of temperature and decreases with increase in rainfall.
As to the sensitivity index of $\bar{\mathcal{R}}_0$ with respect to temperature, we can see that, as temperature increases the sensitivity index of $\bar{\mathcal{R}}_0$ with respect to temperature decreases from positive values to become negative beyond 28.8 C^o. This confirms what we already know that increasing temperature from low to mild values is more favorable for the spread of malaria, while increasing it from higher values would

reduce the speared of malaria. Lastly, the sensitivity index of $\bar{\mathcal{R}}_0$ with respect to temperature does not significantly change with rainfall.

3.4.3. *Existence of backward bifurcation in the autonomous version of the model*

At the steady states of the autonomous version of (2.4) which is calculated by equating its right side to zero, the zero force of infection corresponds to the disease-free periodic solution (DFPS) of the autonomous version and the non zero force of infection $\lambda_h^* = \frac{\beta_{vh}\phi I_v^*}{N_h^*}$ satisfies the quadratic equation

$$A{\lambda^*}_h^2 + B\lambda_h^* + C = 0 \tag{3.12}$$

where $A = (\kappa + r_h)\left(\mu_v(\kappa + r_h) + \beta_{hv}\phi\kappa\right)\Lambda_h$,

$B = \dfrac{\left(\mu_h\gamma + \sigma(\mu_h + \mu_d)\right)\kappa\gamma\mu_v\Lambda_h}{\mu_h}(K - \bar{\mathcal{R}}_0^2)$ and $C = \kappa^2\gamma^2\mu_v\Lambda_h(1 - \bar{\mathcal{R}}_0^2)$ with

$K = \frac{\mu_h(\beta_{hv}\phi + 2(\kappa + r_h))}{(\mu_h\gamma + \sigma(\mu_h + \mu_d))\mu_v}$, $\gamma = \mu_h + r_h + \mu_d$ and $\kappa = \mu_h + \sigma$.

We have the following results:

Proposition 3.6.

(1) If $K \geq 1$, then the autonomous version of (2.4) exhibits transcritical bifurcation.

(2) If $K < 1$, then the autonomous version of (2.4) exhibits backward bifurcation. That is, there exists $\bar{\mathcal{R}}_c$ in (0,1) such that

- ***i.*** *If $1 \leq \bar{\mathcal{R}}_0$ then the autonomous version of (2.4) has one endemic equilibrium point.*
- ***ii.*** *If $\bar{\mathcal{R}}_c < \bar{\mathcal{R}}_0 < 1$ then the autonomous version of (2.4) has two endemic equilibrium points.*
- ***iii.*** *If $\bar{\mathcal{R}}_0 = \bar{\mathcal{R}}_c$ then the autonomous version of (2.4) has one endemic equilibrium point.*
- ***iv.*** *If $\bar{\mathcal{R}}_0 < \bar{\mathcal{R}}_c$ then the autonomous version of (2.4) has no endemic equilibrium points.*

Note that $K < 1$ if and only if

$$(2\mu_h - \mu_v(\mu_d + \mu_h))\sigma < \mu_h(\mu_v(\mu_h + r_h + \mu_d) - (2\mu_h + 2r_h + \phi\beta_{hv}))$$

That is

$$\sigma < \frac{\mu_h(\mu_v(\mu_h + r_h + \mu_d) - (2\mu_h + 2r_h + \phi\beta_{hv}))}{(2\mu_h - \mu_v(\mu_d + \mu_h))} \text{ if } 2\mu_h > \mu_v(\mu_d + \mu_h)$$

or

$$\sigma > \frac{\mu_h(\mu_v(\mu_h + r_h + \mu_d) - (2\mu_h + 2r_h + \phi\beta_{hv}))}{(2\mu_h - \mu_v(\mu_d + \mu_h))} \text{ if } 2\mu_h < \mu_v(\mu_d + \mu_h)$$

The fact that the model exhibits a backward bifurcation when the parameters are constant is well known in many of the literatures (see for example [22], [20], [3]). However, when some of the parameters themselves are made to be time dependent, no such phenomenon (like backward bifurcation) is established yet. In the contrary, as can be mentioned in the next subsection, it has been asserted that the disease free equilibrium no longer exists and we have instead a disease free solution (DFS) which is globally asymptotically stable when $\tilde{\mathcal{R}}_{no}(t)$ is less than unity. This could be due to the structure of the DFS and the definition of the threshold trajectory $\tilde{\mathcal{R}}_{no}(t)$.

The mathematical analyses above are dedicated to the case where the temperature and rainfall are assumed to be cyclic or constant. However, the actual malaria confirmed cases in the Asendabo region, a western region of Ethiopia, in the years 2000-2012 and is plotted against time in months (Fig. 4) shows that the incidence pattern does not follow a periodic flow. So, it is more appealing to formulate and analyze a non-autonomous model system in the non-periodic environment for the epidemic.

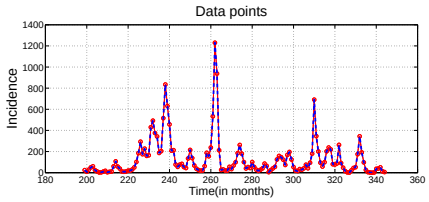

Fig. 6: The actual malaria confirmed cases in the Asendabo region, collected in the years 2000-2012.

3.5. *Non-periodic System*

The climate impact upon the distribution of the malaria transmission in space and time is not always periodical and we need to investigate the potential change in malaria risk caused by the variations in temperature and rainfall in the general case. That is, when these climate variables are any time dependent functions. This may help to investigate the dynamics of the disease in a long term basis and the information provided here might serve as an important contribution for strategic planning of malaria control in a long period of time in the future. From the observed rainfall data as the variation of rainfall looks too seasonal and hence nearly periodic, the non-periodic fit does not give a better fit than the periodic fit. For this reason, the present section is devoted to studying the dynamics of the disease with parameters dependent on the non-periodic climate variable (temperature) and the periodic climate variable (rainfall).

Even though the climate variables (temperature and rainfall) values change seasonally, they are not totally periodic and hence it is very important to investigate the dynamics in the non-periodic environment too. For the general case, that is, for the general climate variables values, we analyze model (2.4) by making the model parameters dependent on the general climate variables. Thus the system will have time dependent non-periodic coefficients as climate variables could be expressed as a function of time.

3.6. *Stability analysis for the non-periodic non-autonomous system*

Consider the second and the fifth equations of (2.4):

$$\begin{aligned}\frac{dI_h}{dt} &= \beta_{vh}\phi(T(t))\frac{S_h}{N_h}I_v - \gamma I_h \leq \beta_{vh}\phi(T(t))I_v - \gamma I_h,\\ \frac{dI_v}{dt} &\leq \beta_{hv}\phi(T(t))\frac{N_v}{N_h}I_h - \mu_v(T(t),R(t))I_v\\ &\leq \beta_{hv}\phi(T(t))\Gamma_v I_h - \mu_v(T(t),R(t))I_v.\end{aligned} \tag{3.13}$$

where $\Gamma_v = \frac{\sup_{t>0}\{\Lambda_v(T(t),R(t))\}}{\inf_{t>0}\{\mu_v(T(t),R(t))\}}$.

We analyze the stability of the disease-free solution $I_v = I_h = 0$, that is, the solution representing the absence of the infection.

Linearizing the system (3.13) around a small amount of disease i_H and i_V as in [8], we get

$$\begin{aligned}\frac{di_H}{dt} &= -\gamma i_H + \beta_{vh}\phi(T(t))i_V,\\ \frac{di_V}{dt} &= \beta_{hv}\phi(T(t))\Gamma_v i_H - \mu_v(T(t),R(t))i_V,\end{aligned} \tag{3.14}$$

We then examine the stability of the disease-free solution of system (3.14), that is, $i_H = 0$ and $i_V = 0$ as if the system were autonomous [8]. For this we assume the solutions:

$$\begin{aligned}i_H &= c_1 exp(\lambda t),\\ i_V &= c_2 exp(\lambda t)\end{aligned} \tag{3.15}$$

and replace (3.15) into equation (3.14). The characteristic equation associated to system (3.14) is then obtained to be:

$$\begin{vmatrix}-(\lambda+\gamma) & \beta_{vh}\phi(T(t))\\ \beta_{hv}\phi(T(t))\Gamma_v & -(\lambda+\mu_v(T(t),R(t)))\end{vmatrix} = 0 \tag{3.16}$$

that is, $\lambda(t) = \frac{1}{2}\left(-(\gamma+\mu_v) \pm \sqrt{(\gamma+\mu_v)^2 - 4(\gamma\mu_v - \beta_{hv}\beta_{vh}\phi^2(T(t))\Gamma_v)}\right)$ where $\mu_v = \mu_v(T(t),R(t))$.

If all the roots of equation (3.16) have negative real parts, then the solution without

disease is stable, that is, the origin is an attractor. We see that the first root that crosses the imaginary axis do so through the real axis and this happens when $\gamma\mu_v(T(t), R(t)) - \beta_{hv}\beta_{vh}\phi^2(T(t))\Gamma_v < 0$ that is when

$$\tilde{\mathcal{R}}_{no}(t) := \frac{\beta_{hv}\beta_{vh}\phi^2(T(t))\Gamma_v}{\gamma\mu_v(T(t), R(t))} > 1.$$

Since $\mu_v(T(t), R(t))$ is never zero, the definition of $\tilde{\mathcal{R}}_{no}$ is meaningful.
Therefore, we can find the time t at which the disease-free solution of system (3.14), that is, $i_H = 0$ and $i_V = 0$ becomes unstable. The time t at which the disease-free solution (no-disease) of the autonomous system becomes unstable ($\tilde{\mathcal{R}}_{no} > 1$) corresponds approximately to the moment at which the epidemic takes off, that is, when the epidemic in system (2.4) begins to increase as a result of the introduction of a small amount of disease at time $t = 0$.

Theorem 3.7. *If $\tilde{\mathcal{R}}_{no}(t) < 1$, for all $t \geq t_0$ then the disease-free solution* (2.10)*, is globally asymptotically stable.*

Proof. From equation (3.13), we have that

$$\begin{aligned} dI_h/dt &\leq \beta_{vh}\phi(T(t))I_v - \gamma I_h \\ dI_v/dt &\leq \beta_{hv}\phi(T(t))\Gamma_v I_h - \mu_v(T(t), R(t))I_v. \end{aligned}$$

Let Y=$\binom{y_1}{y_2}$ be the solution of

$$\mathbf{Y}' = \begin{pmatrix} -\gamma + \varepsilon & \beta_{vh}\phi(T(t)) \\ \beta_{hv}\phi(T(t))\Gamma_v & -\mu_v(T(t), R(t)) + \varepsilon \end{pmatrix} Y \tag{3.17}$$

with $y_1(0) = I_h(0) + \varepsilon, y_2(0) = I_v(0) + \varepsilon,\ \varepsilon > 0$.
From the argument above this Theorem 3.7, we see that the solutions of (3.17) are characterized by:

$$y_1(t) \longrightarrow 0 \ \text{ and } \ y_2(t) \longrightarrow 0 \ \text{ as } \ t \longrightarrow \infty. \tag{3.18}$$

We claim that

$$I_h(t) < y_1(t) \ \text{ and } \ I_v(t) < y_2(t) \ \text{ for all } \ t > 0. \tag{3.19}$$

Indeed, otherwise there exists a first point $t = t_0 > 0$ such that either $I_h(t_0) = y_1(t_0)$ or $I_v(t_0) = y_2(t_0)$. Suppose that the first case occurs. Then
$\dot{y}_1(t_0) = \beta_{vh}\phi(t_0)y_2(t_0) - \gamma y_1(t_0) + \varepsilon y_1(t_0) > \beta_{vh}\phi(t_0)\frac{S_h}{N_h}I_v(t_0) - \gamma I_h(t_0) = \dot{I}_h(t_0)$.
On the other hand, since $y_1(t) - I_h(t) > 0$ for $t < t_0$ and $y_1(t_0) - I_h(t_0) = 0$, we obtain $\dot{y}_1(t_0) - \dot{I}_h(t_0) \leq 0$, which is a contradiction. The case $I_v(t_0) = y_2(t_0)$ can be handled in the same way.
Letting $t \to \infty$ in equation (3.19) and using equation (3.18), we conclude that $I_h(t) \to 0,\ \ I_v(t) \to 0$ if $t \to \infty$. It remains to show that $\lim_{t\to\infty} S_h(t) = N_h$.

From the system (2.4), $\frac{d(N_h - S_h)}{dt} + \kappa(N_h - S_h) = \rho(t)$, where $\rho(t) = (\sigma - \mu_d)I_h + \beta_{vh}\phi(T(t))S_h\frac{I_v}{N_h}$ and $\kappa = \mu_h + \sigma$.

$$\begin{aligned} N_h(t) - S_h(t) &= exp\left(-\int_0^t \kappa d\tau\right)\left\{(N_h(0) - S_h(0)) + \int_0^t \rho(s)exp(\int_0^s \kappa d\sigma)ds\right\} \\ &= exp\left(-\kappa t\right)\left\{(N_h(0) - S_h(0)) + \int_0^t \rho(s)exp(\kappa s)ds\right\} \end{aligned}$$

Since $\rho(t) \to 0$ as $t \to \infty$, we can find $t_M > 0$ such that $\rho(t) \leq Me^{-\kappa t}$ for some constant M and $t > t_M$. Hence

$$\begin{aligned} \lim_{t\to\infty} exp(-\kappa t)\int_0^t \rho(s)exp(\kappa s)ds &\leq \lim_{t\to\infty} exp(-\kappa t)\left(\int_0^{t_M} \rho(s)exp(\kappa s)ds + \int_{t_M}^t Mds\right) \\ &= \lim_{t\to\infty} exp(-\kappa t)\left([\int_0^{t_M} \rho(s)exp(\kappa t)ds - Mt_M] + Mt\right) \\ &= \lim_{t\to\infty} exp(-\kappa t)(M_0 + Mt) = 0 \end{aligned}$$

letting the constant $\int_0^{t_M} \rho(s)exp(\kappa s)ds - Mt_M$ to be M_0 and by L'Hôpital's rule. Thus $\lim_{t\to\infty}(N_h(t) - S_h(t)) = 0$. That is $S_h(t) \to N_h(t)$ as $t \to \infty$. □

Theorem 3.8. *If $\tilde{\mathcal{R}}_{no}(t) > 1$ for all $t \geq t_0$ then the nonlinear system (2.4) is uniformly persistent, that is, there exists $c > 0$ (independent of initial conditions), such that $\liminf_{t\to\infty} I_h \geq c$ and $\liminf_{t\to\infty} I_v \geq c$.*

Proof. Consider the second and the fourth equation of the nonlinear system (2.4)

$$\begin{aligned} dI_v/dt &= -\mu_v(T(t), R(t))I_v + \frac{\beta_{hv}\phi(T(t))S_v}{N_h}I_h. \\ dI_h/dt &= \frac{\beta_{vh}\phi(T(t))S_h}{N_h}I_v - \gamma I_h \end{aligned}$$

and written in matrix form as

$$\mathbf{I}' = \begin{pmatrix} -\mu_v & \lambda_v \\ \lambda_h & -\gamma \end{pmatrix}\mathbf{I} = A(t)\mathbf{I} \tag{3.20}$$

where $\mathbf{I}=\binom{I_v}{I_h}$, $\mu_v = \mu_v(T(t), R(t))$, $\lambda_v = \frac{\beta_{hv}\phi(T(t))S_v}{N_h}$ and $\lambda_h = \frac{\beta_{vh}\phi(T(t))S_h}{N_h}$.
The eigenvalues of A are $\ell(t) = \frac{1}{2}\left(-(\gamma + \mu_v) \pm \sqrt{(\gamma + \mu_v)^2 - 4(\gamma\mu_v - \lambda_h\ell_v)}\right)$.
Since all the components of our square-matrix function $A(t)$ are real analytic functions of t, then it is already known that all its eigenvalues and the corresponding eigenvectors are also real analytic functions of t (see Chapter 9 of [15]).

Now $\ell(t) > 0$ for all $t > 0$ when $\gamma\mu_v - \lambda_h\lambda_v < 0$ which implies

$$1 < \frac{\lambda_h\lambda_v}{\gamma\mu_v} = \frac{\beta_{hv}\phi(T(t))S_v}{N_h}\frac{\beta_{vh}\phi(T(t))S_h}{N_h}\frac{1}{\gamma\mu_v} \leq \frac{\beta_{hv}\beta_{vh}\phi(T(t))^2}{\gamma\mu_v}S_v$$

$$\leq \frac{\beta_{hv}\beta_{vh}\phi(T(t))^2}{\gamma\mu_v}\Gamma_v = \tilde{\mathcal{R}}_{no}(t).$$

One right-eigenvector function corresponding to $\ell(t) > 0$ is $v(t) = \left(\frac{1}{\frac{\mu_v+\ell(t)}{\lambda_v}}\right)$ and

$$\mathbf{I} = \begin{pmatrix} I_v \\ I_h \end{pmatrix} = c\begin{pmatrix} 1 \\ \frac{\mu_v+\ell(t)}{\lambda_v} \end{pmatrix} e^{\ell(t)t} \quad \text{is the solution of (3.20).}$$

So $I_v(t) = ce^{\ell(t)t}$ and

$$I_h(t) = c\left(\frac{\mu_v+\ell(t)}{\lambda_v}\right)e^{\ell(t)t} = c\left(\frac{(\mu_v+\ell(t))N_h}{\beta_{hv}\phi(T(t))S_v}\right)e^{\ell(t)t} \geq c\left(\frac{(\mu_v+\ell(t))N_h}{\beta_{hv}\phi(T(t))N_v}\right)e^{\ell(t)t}$$

Now for an eigenvalue function $\ell(t) > 0$ for all $t > 0$, which is a real analytic function, the corresponding solution function $I = \binom{I_v}{I_h} = c\binom{1}{v(t)}e^{\ell(t)t}$ is a smooth function of t and the limit of the exponential function increases indefinitely as t increases. This completes the proof. □

4. Numerical Simulations

The numerical simulation of the non-autonomous model (2.4) is used to illustrate the impact of the seasonal variables (temperature and rainfall) on the malaria disease dynamics in a population and to validate the model results in the real situation on the ground.

In this section, we give numerical simulations to confirm the above theoretical analysis in the real situation in Ethiopia. For this purpose, the daily temperature and rainfall data is taken from the National Meteorological Agency of Ethiopia and the corresponding microscopically confirmed cases of malaria from 1984-2012 for Asendabo, a western region of Ethiopia, is obtained from Asendabo clinic.

For the simulation, the monthly average maximum temperature and the average monthly rainfall is used to show their impact on the incidence and prevalence of the malaria disease in the region. The temperature raw data is fitted by both periodic(Fig. 7) and non-periodic(Fig. 8) functions, respectively, by

$$T(t) = 19.5932 + 1.2697\cos(0.5240t + 4.3391) - 0.6343\cos(2*0.5240t - 0.6963) \quad (4.1)$$

$$T(t) = 29.2446 + 0.0018t + 2.5535\cos(0.5237t + 5.0431) - 0.5624\cos(2*0.5237t - 1.101) \quad (4.2)$$

while the rainfall raw data is fitted by a periodic function(Fig. 9) only as the raw rainfall data seems very much periodic.

$$\begin{aligned} R(t) =& 99.4876 + 89.8581\cos(0.5232t + 15.4500) + 19.1069\sin(2 * 0.5232t) \\ & -8.5891\cos(3 * 0.5232t + 3.7723) + 6.4660\sin(5 * 0.5232t). \end{aligned} \quad (4.3)$$

It is assumed that initially, the susceptible and infected adult mosquitoes are $S_v(0) = 800000$, $I_v(0) = 8000$ and the host population distributions are $S_h(0) =$

20000, $I_h(0) = 500$, $R_h(0) = 50$, respectively.

Table 2: Parameter values used in all the simulations.

Parameter	Estimated value	Reference
Λ_h	0.415244 day^{-1}	[6]
σ	0.00137 day^{-1}	[7]
μ_h	0.0000388 day^{-1}	[6]
μ_d	0.00047 day^{-1}	[26]
β_{vh}	0.24 day^{-1}	[23]
β_{hv}	0.022 day^{-1}	[23]
r_h	0.0028 day^{-1}	[23]

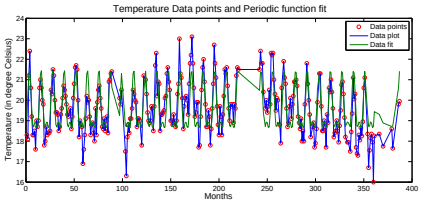

Fig. 7: Monthly average maximum temperature raw data periodic fit.

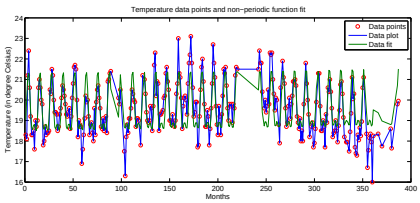

Fig. 8: Monthly average maximum temperature raw data non-periodic fit.

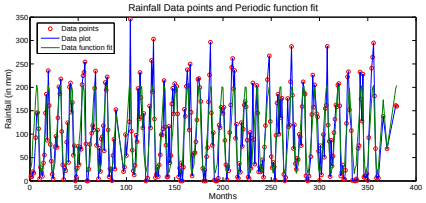

Fig. 9: Monthly average rainfall raw data periodic fit.

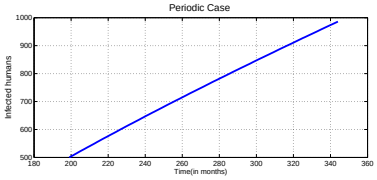

Fig. 10: Infected humans in the periodic case.

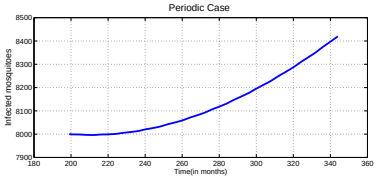

Fig. 11: Infected mosquitoes in the periodic case.

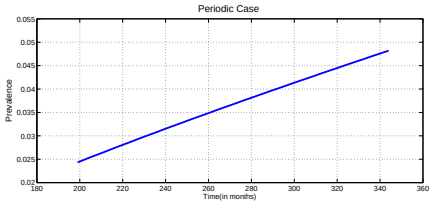

Fig. 12: Prevalence in the periodic case.

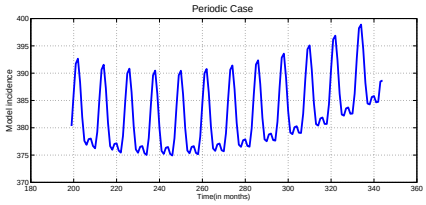

Fig. 13: The model disease incidence in the periodic case.

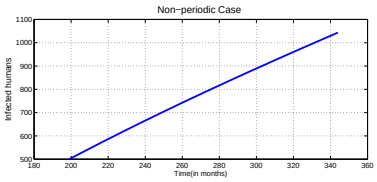

Fig. 14: Infected humans in the non-periodic case.

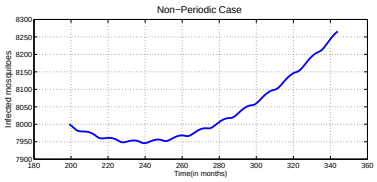

Fig. 15: Infected mosquitoes in the non-periodic case.

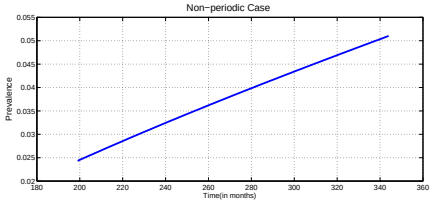

Fig. 16: Prevalence in the non-periodic case.

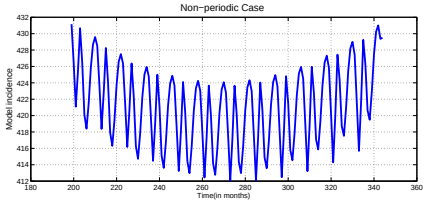

Fig. 17: The model disease incidence in the non-periodic case.

The need for studying the dynamical system in the non-periodic environment is to fill the gap ignored by studying the system in the periodic environment only. To show this a non-periodic fit for the temperature data (Fig.8) only is used while the rainfall data fit is kept periodic. The time series simulations of infected humans and infected mosquitoes have shown noticeable variations in the periodic and non-

periodic environments as shown (Figures 10, 11, 14 and 15). With this non-periodic temperature data fit obtained by a slight modification of the periodic temperature data fit only, the disease prevalence and the corresponding model incidence in the non-periodic case have shown some change in their behavior when compared to the periodic case. The prevalence rate of increase is 105.1% in the non-periodic environment while it is 94.2% in the periodic environment and the model incidence in the non-periodic case ranges from 412 to 432 in the non-periodic case (Fig. 17) while it ranges from 375 to 400 (Fig. 13) in the periodic case in the time range between the 200^{th} month and the 340^{th} month. This basic difference is a consequence of analyzing the model in both environments and it may be a good reason to study the malaria dynamics in the non-periodic environment besides the periodic one.

Remark 4.1. Note here that there were no control interventions assumed to have been implemented in both periodic and non-periodic environments in the given period of time, and the model produces the dynamics of the disease if no intervention were employed.

It is known that by employing control interventions such as spraying chemicals, destroying some breading sites and using Insecticide Treated bed-nets (ITBNs) the mortality rate of the vectors can be increased and using ITBNs at the household level effectively, the biting rate of mosquitoes can be reduced significantly.

We have investigated and compared numerical results from simulations with three scenarios under the assumption that appropriate control interventions are employed.

i. If it is possible to reduce the biting rate by 50% and increase the mortality rate of the vectors by 30%, it is seen that a 20.4% (Fig.38) reduction of the prevalence in the periodic case and a 21.8% (Fig.24) reduction of the prevalence in the non-periodic case can be achieved. The corresponding incidence declines are shown in Fig.39 in the periodic case and in Fig.25 in the non-periodic case.
ii. If the mortality rate of the vectors only is increased by 50%, a 0.64% (Fig.28) reduction of the prevalence in the periodic case and a 1.4% (Fig.32) reduction of the prevalence in the non-periodic case can be achieved.
iii. If the biting rate only is reduced by 50%, a 20.1% (Fig.36) reduction of the prevalence in the periodic case and a 21.4% (Fig.40) reduction of the prevalence in the non-periodic case can be achieved.

5. Conclusions

We derived and analyzed a deterministic non-autonomous model for the transmission of malaria disease in a periodic and non-periodic environments. We calculated the basic reproduction ratios in the periodic environment and the threshold function in the non-periodic environment and investigated the existence and stability of

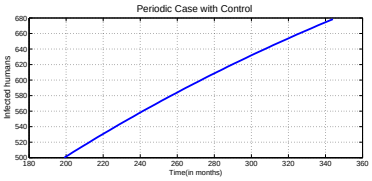

Fig. 18: Infected humans in the periodic case with control in the first scenario.

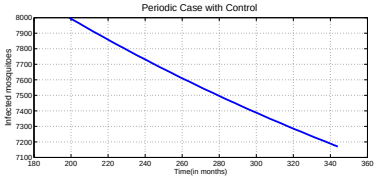

Fig. 19: Infected mosquitoes in the periodic case with control in the first scenario.

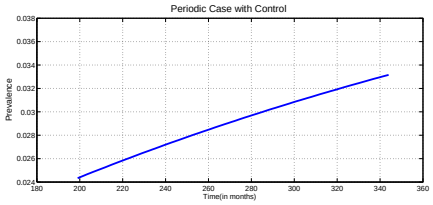

Fig. 20: Prevalence with control in the periodic case in the first scenario.

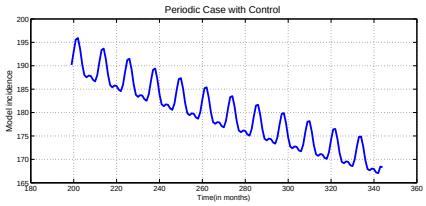

Fig. 21: The model disease incidence in the periodic case with control in the first scenario.

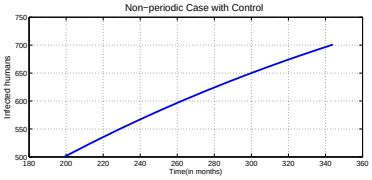

Fig. 22: Infected humans in the non-periodic case with control in the first scenario.

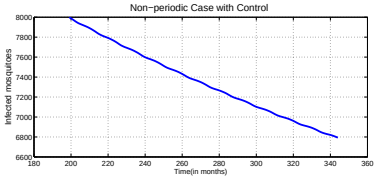

Fig. 23: Infected mosquitoes in the non-periodic case with control in the first scenario.

equilibria in both environments. The dynamics of mosquito populations are driven by climatic factors, rainfall and temperature.

The impact of these climatic variables, temperature and rainfall, in both environments is investigated and the corresponding model parameters are shown to be influenced by these climate variables. The model results have been validated using epidemiological data obtained from a western region of Ethiopia, by considering the trends for monthly microscopically confirmed cases of malaria during the years 2000-2012 and the corresponding climate variation in the region. In both environments, it has been shown that the model incidence result increases slowly until it

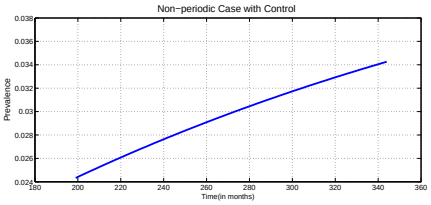

Fig. 24: Prevalence with control in the non-periodic case in the first scenario.

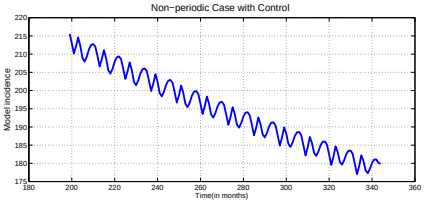

Fig. 25: The model disease incidence in the non-periodic case with control in the first scenario.

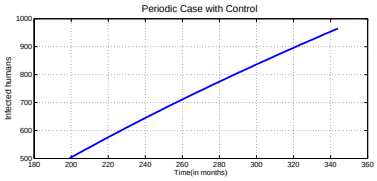

Fig. 26: Infected humans in the periodic case with control in the second scenario.

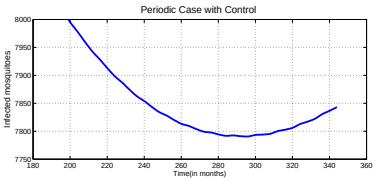

Fig. 27: Infected mosquitoes in the periodic case with control in the second scenario.

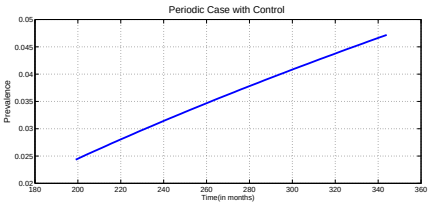

Fig. 28: Prevalence in the periodic case with control in the second scenario.

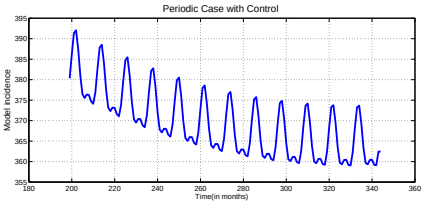

Fig. 29: The model disease incidence in the periodic case with control in the second scenario.

reaches a point where it tends to stop rising in the absence of implementation of any kind of control measures and the actual incidence is a result of some control interventions implemented in the country in these years. This shows that the climate variables have significant impact on the disease dynamics and proper implementation of control measures is required to achieve a significant reduction of the malaria disease dynamics.

When our model is reduced to its autonomous version, the fact that the model exhibit a backward bifurcation is well known in many of the literatures and our

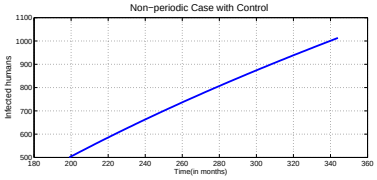

Fig. 30: Infected humans in the non-periodic case with control in the second scenario.

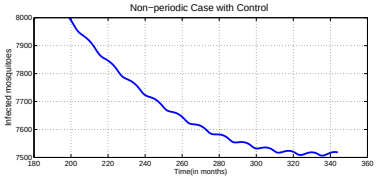

Fig. 31: Infected mosquitoes in the non-periodic case with control in the second scenario.

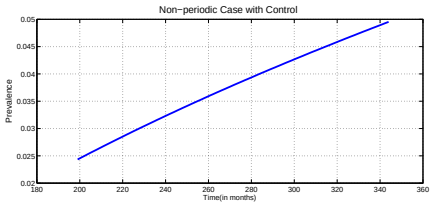

Fig. 32: Prevalence in the non-periodic case with control in the second scenario.

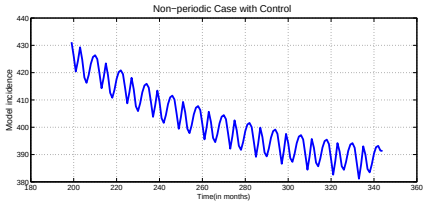

Fig. 33: The model disease incidence in the non-periodic case with control in the second scenario.

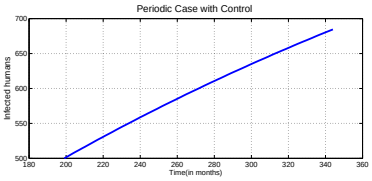

Fig. 34: Infected humans in the periodic case with control in the third scenario.

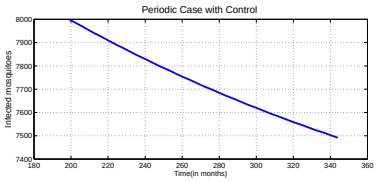

Fig. 35: Infected mosquitoes in the periodic case with control in the third scenario.

model also reduces to the same phenomena. However, when some of the parameters themselves are made to be time dependent, no such phenomenon (like backward bifurcation) is established yet. In the contrary it has been asserted that the DFS is globally asymptotically stable when the basic reproduction number $\bar{R}_0$ is less than unity. This looks a bit strange and needs to be investigated but the mathematical argument clearly shows that our model also satisfies this characterization.

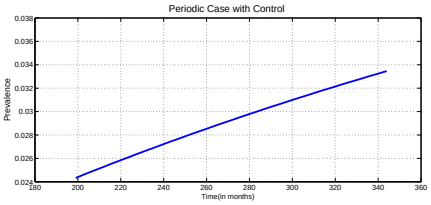

Fig. 36: Prevalence with control in the periodic case in the third scenario.

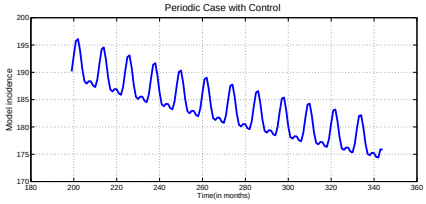

Fig. 37: The model disease incidence in the periodic case with control in the third scenario.

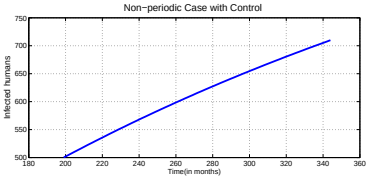

Fig. 38: Infected humans in the non-periodic case with control in the third scenario.

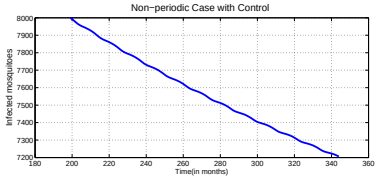

Fig. 39: Infected mosquitoes in the non-periodic case with control in the third scenario.

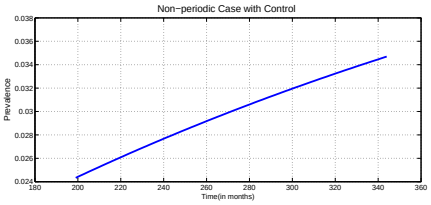

Fig. 40: Prevalence in the non-periodic case with control in the third scenario.

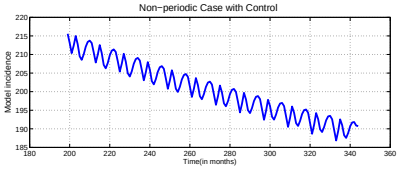

Fig. 41: The model disease incidence in the non-periodic case with control in the third scenario.

6. Appendix

6.1. *Proof of Proposition 3.1 (the well-posedness property of the model)*

Denote by t_{max} the upper bound of the maximum interval of existence corresponding to
$(S_v(t), I_v(t), S_h(t), I_h(t), R_h(t))$. We first note that if we show that the solution is positive and bounded in $[0, t_{max})$, then the solution would be positive and bounded in $[0, +\infty)$. Let

$$t_1 = \sup\left\{0 \leq t < t_{max} : S_v(\tau), I_v(\tau), S_h(\tau), I_h(\tau) \text{ and } R_h(\tau) \text{ are positive for all } \tau \in [0, t]\right\}.$$

Since $S_v(0), I_v(0), S_h(0), I_h(0)$ and $R_h(0)$ are non-negative then $t_1 > 0$. If $t_1 < t_{max}$ then, by using the variation of constants formula to the first equation of system (2.4), we have

$$\begin{aligned} S_v(t_1) = S_v(0)e^{-\int_0^{t_1}(\lambda_v(T(\tau))+\mu_v(T(\tau),R(\tau)))d\tau} \\ + \int_0^{t_1} e^{-\int_s^{t_1}(\lambda_v(T(\tau))+\mu_v(T(\tau),R(\tau)))d\tau}\Lambda_v(T(s),R(s))\,ds. \end{aligned}$$

Since $S_v(0) \geq 0$ and $\Lambda_v(T(s),R(s)) \geq 0$ for all $s \in [0,t_1)$, then $S_v(t_1) > 0$. Similarly, we have

$$\begin{aligned} I_v(t_1) = I_v(0)e^{-\int_0^{t_1}\mu_v(T(\tau),R(\tau))d\tau} \\ + \int_0^{t_1} e^{-\int_s^{t_1}\mu_v(T(\tau),R(\tau))d\tau}\lambda_v(T(s))\,S_v(s)\,ds. \end{aligned}$$

which by $I_v(0) \geq 0$ and $\lambda_v(T(s))\,S_v(s) \geq 0$ for all $s \in [0,t_1)$, imply that $I_v(t_1) > 0$. It can be shown in the same manner that the other variables are also positive at t_1. This contradicts the topological property of the supremum that states that at least one of the variables should be equal to zero at t_1. Therefore our assumption $t_1 < t_{max}$ is false and $t_1 = t_{max}$ which implies that the solution is positive on its maximal interval of existence $[0, t_{max})$.
Next, to show that the solution is bounded on $[0, t_{max})$, we obtain from the first two equations of system (2.4)

$$\dot{N}_v(t) = \Lambda_v(T(t),R(t)) - \mu_v(T(t),R(t))\,N_v(t).$$

By using the standard comparison theorem [14] and by accounting for the positivity of the solution on $[0, t_{max})$, we obtain

$$N_v(t) = e^{-\int_0^t \mu_v(T(\tau),R(\tau))d\tau}\left(N_v(0) + \int_0^t \Lambda_v(T(s),R(s))\,e^{\int_0^s \mu_v(T(\tau),R(\tau))d\tau}ds\right)$$

for any $0 \leq t < t_{\max}$. Since for all $x \geq 0$, we have $\mu_v(T(x),R(x)) \geq m_v$ and $\Lambda_v(T(x),R(x)) \leq M_v$, then

$$N_v(t) \leq e^{-m_v t}\left(N_v(0) + \frac{M_v}{m_v}\left(e^{m_v t} - 1\right)\right). \tag{6.1}$$

Thus $N_v(t)$ is bounded on $[0, t_{max})$.
Similarly, by adding equations four, five and six of system (2.4), we have

$$\begin{aligned} \dot{N}_h(t) &= \Lambda_h - \mu_h N_h(t) - \mu_d I_h(t) \\ &\leq \Lambda_h - \mu_h N_h(t) \end{aligned}$$

The standard comparison theorem [14] and the positivity of the solution on $[0, t_{max})$ yield

$$\begin{aligned} N_h(t) &\leq e^{-\int_0^t \mu_h d\tau}\left\{N_h(0) + \int_0^t \Lambda_h e^{\int_0^s \mu_h d\tau}ds\right\} \leq e^{-\mu_h t}N_h(0) + \Lambda_h e^{-\mu_h t}\int_0^t e^{\mu_h s}ds \\ &\leq e^{-\mu_h t}\left(N_h(0) - \tfrac{\Lambda_h}{\mu_h}\right) + \tfrac{\Lambda_h}{\mu_h}. \end{aligned} \tag{6.2}$$

for any $0 \leq t < t_{\max}$. Thus we obtain

$$N_h(t) \leq \frac{\Lambda_h}{\mu_h} \text{ for all } t \in [0, t_{\max}), \tag{6.3}$$

Thus $N_h(t)$ is also bounded on $[0, t_{max})$. Hence $t_{max} = \infty$ which proves the global existence, the positivity and the boundedness results.
Concerning the invariance properties, it is easy to obtain from (6.1) that if $N_v(0) \leq \frac{M_v}{m_v}$, then $N_v(t) \leq \frac{M_v}{m_v}$ for all $t \geq 0$. Similarly, from (6.2) we obtain that if $N_h(0) \leq \frac{\Lambda_h}{\mu_h}$ then $N_h(t) \leq \frac{\Lambda_h}{\mu_h}$. This establishes the invariance property as required. □

6.2. *Proof of Proposition 3.6 (the bifurcation results)*

(1) If $K \geq 1$, we have the following

- **i.** If $\bar{\mathcal{R}}_0 > 1$, then $C < 0$. In this case the autonomous version of (2.4) has a unique positive solution.
- **ii.** If $\bar{\mathcal{R}}_0 \leq 1$, then $C \geq 0$ and $B \geq 0$ (because $\bar{\mathcal{R}}_0 \leq 1 \leq \sqrt{K}$). This together with $A > 0$ imply that the autonomous version of (2.4) has no positive solution.

(2) If $K < 1$, we have

- **i.** If $\bar{\mathcal{R}}_0 \geq 1$, then $C \leq 0$ which implies that the autonomous version of (2.4) has a unique positive solution.
- **ii.** If $\bar{\mathcal{R}}_0 \leq \sqrt{K}$, then $B \geq 0$ and $C > 0$. This implies that the autonomous version of (2.4) has no positive solution.
- **iii.** If $\sqrt{K} < \bar{\mathcal{R}}_0$, we consider the discriminant of (3.12) $\triangle(\bar{\mathcal{R}}_0) := B^2 - 4AC$. We note that $\triangle(\sqrt{K}) := -4AC < 0$ and $\triangle(1) := B^2 > 0$. Therefore, there exists $\bar{\mathcal{R}}_c \in (\sqrt{K}, 1)$ such that $\triangle(\bar{\mathcal{R}}_c) = 0$ and $\triangle < 0$ for $\bar{\mathcal{R}}_0 \in (\sqrt{K}, \bar{\mathcal{R}}_c)$ and $\triangle > 0$ for $\bar{\mathcal{R}}_0 \in (\bar{\mathcal{R}}_c, 1)$. In this case we have
  a. If $\sqrt{K} < \bar{\mathcal{R}}_0 < \bar{\mathcal{R}}_c$ then (3.12) has no positive solution.
  b. If $\bar{\mathcal{R}}_0 = \bar{\mathcal{R}}_c$ then $\triangle = 0$ and $B < 0$. This implies that (3.12) has one positive solution.
  c. If $\bar{\mathcal{R}}_c < \bar{\mathcal{R}}_0 < 1$ then (3.12) has two real solutions which are positive since $C > 0$ and $B < 0$. □

Acknowledgments

The first author thanks the Department of Mathematics at Addis Ababa University and the International Science Program (ISP) for financial support and the DST/NRF Centre of Excellence in Epidemiological Modelling and Analysis (SACEMA) at Stellenbosch University, South Africa for scholarly assistance he received during the preparation of this manuscript. The authors acknowledge with thanks the Asendabo Health Center for their support on epidemiological data collection and the National Meteorological Agency of Ethiopia for providing the climate

data requested. The authors would also like to thank editor and the two anonymous referees of this journal from whom we received valuable comments and suggestions to improve the earlier version of the manuscript. The third author acknowledges the support from the DST/NRF SARChI Chair in Mathematical Models and Methods in Biosciences and Bioengineering at the University of Pretoria □

References

[1] A. Abdelrazec and A. B. Gumel. Mathematical assessment of the role of temperature and rainfall on mosquito population dynamics. *Journal of mathematical biology*, 74(6):1351–1395, 2017.

[2] F. Agusto, A. Gumel, and P. Parham. Qualitative assessment of the role of temperature variations on malaria transmission dynamics. *Journal of Biological Systems*, 23(04):1550030, 2015.

[3] F. B. Agusto, S. Y. Del Valle, K. W. Blayneh, C. N. Ngonghala, M. J. Goncalves, N. Li, R. Zhao, and H. Gong. The impact of bed-net use on malaria prevalence. *Journal of theoretical biology*, 320:58–65, 2013.

[4] D. Alonso, M. J. Bouma, and M. Pascual. Epidemic malaria and warmer temperatures in recent decades in an east african highland. *Proceedings of the Royal Society B: Biological Sciences*, 278(1712):1661–1669, 2010.

[5] L. M. Beck-Johnson, W. A. Nelson, K. P. Paaijmans, A. F. Read, M. B. Thomas, and O. N. Bjørnstad. The effect of temperature on anopheles mosquito population dynamics and the potential for malaria transmission. *PLOS one*, 8(11):e79276, 2013.

[6] C. Bielli, G. Berhanu, A. Isaias, and A. Orasi. *Population growth and environment in Ethiopia*. CSA, 2001.

[7] K. Blayneh, Y. Cao, and H.-D. Kwon. Optimal control of vector-borne diseases: treatment and prevention. *Discrete and Continuous Dynamical Systems B*, 11(3):587–611, 2009.

[8] F. A. Coutinho, M. N. Burattini, L. F. Lopez, and E. Massad. An approximate threshold condition for non-autonomous system: an application to a vector-borne infection. *Mathematics and Computers in simulation*, 70(3):149–158, 2005.

[9] M. H. Craig, R. Snow, and D. le Sueur. A climate-based distribution model of malaria transmission in sub-saharan africa. *Parasitology today*, 15(3):105–111, 1999.

[10] O. Diekmann, J. A. P. Heesterbeek, and J. A. Metz. On the definition and the computation of the basic reproduction ratio R_0 in models for infectious diseases in heterogeneous populations. *Journal of mathematical biology*, 28(4):365–382, 1990.

[11] T. Garske, N. M. Ferguson, and A. C. Ghani. Estimating air temperature and its influence on malaria transmission across africa. *PloS one*, 8(2):e56487, 2013.

[12] A. K. Githeko and W. Ndegwa. Predicting malaria epidemics in the kenyan highlands using climate data: a tool for decision makers. *Global change and human health*, 2(1):54–63, 2001.

[13] M. B. Hoshen and A. P. Morse. A model structure for estimating malaria risk. In W. Takken, P. Martens, and R. J. Bogers, editors, *Environmental Change and Malaria Risk: Global and Local Implications*, volume 9, pages 41–50. Springer, 2005.

[14] V. Lakshmikantham, S. Leela, and A. A. Martynyuk. *Stability Analysis of Nonlinear Systems*. Marcel Dekker, New York, 1989.

[15] P. D. Lax. *Linear algebra and its applications*. John Willey & Sons, 2007.

[16] L. Liu, X.-Q. Zhao, and Y. Zhou. A tuberculosis model with seasonality. *Bulletin of Mathematical Biology*, 72(4):931–952, 2010.

[17] S. Mandal, R. R. Sarkar, and S. Sinha. Mathematical models of malaria-a review. *Malaria journal*, 10(1):1–19, 2011.

[18] W. Martens, L. W. Niessen, J. Rotmans, T. H. Jetten, and A. J. McMichael. Potential impact of global climate change on malaria risk. *Environmental health perspectives*, 103(5):458–464, 1995.

[19] Y. Nakata and T. Kuniya. Global dynamics of a class of seirs epidemic models in a periodic environment. *Journal of Mathematical Analysis and Applications*, 363(1):230–237, 2010.

[20] E. Ngarakana-Gwasira, C. Bhunu, and E. Mashonjowa. Assessing the impact of temperature on malaria transmission dynamics. *Afrika Matematika*, 25(4):1095–1112, 2014.

[21] E. Ngarakana-Gwasira, C. Bhunu, M. Masocha, and E. Mashonjowa. Assessing the role of climate change in malaria transmission in africa. *Malaria research and treatment*, 2016, 2016.

[22] K. O. Okosun, O. Rachid, and N. Marcus. Optimal control strategies and cost-effectiveness analysis of a malaria model. *BioSystems*, 111(2):83–101, 2013.

[23] K. Okuneye and A. B. Gumel. Analysis of a temperature-and rainfall-dependent model for malaria transmission dynamics. *Mathematical biosciences*, 287:72–92, 2017.

[24] J. A. Omumbo, B. Lyon, S. M. Waweru, S. J. Connor, and M. C. Thomson. Raised temperatures over the kericho tea estates: revisiting the climate in the east african highlands malaria debate. *Malaria Journal*, 10(1):12, 2011.

[25] E. A. Onyango, O. Sahin, A. Awiti, C. Chu, and B. Mackey. An integrated risk and vulnerability assessment framework for climate change and malaria transmission in east africa. *Malaria journal*, 15(1):551, 2016.

[26] W. H. Organization, UNICEF, et al. *Achieving the malaria MDG target: reversing the incidence of malaria 2000-2015*. World Health Organization, 2015.

[27] K. P. Paaijmans, S. Blanford, A. S. Bell, J. I. Blanford, A. F. Read, and M. B. Thomas. Influence of climate on malaria transmission depends on daily temperature variation. *Proceedings of the National Academy of Sciences*, 107(34):15135–15139, 2010.

[28] P. E. Parham and E. Michael. Modeling the effects of weather and climate change on malaria transmission. *Environmental health perspectives*, 118(5):620–626, 2009.

[29] P. E. Parham and E. Michael. Modelling climate change and malaria transmission. In *Modelling Parasite Transmission and Control*, pages 184–199. Springer, 2010.

[30] P. E. Parham, D. Pople, C. Christiansen-Jucht, S. Lindsay, W. Hinsley, and E. Michael. Modeling the role of environmental variables on the population dynamics of the malaria vector anopheles gambiae sensu stricto. *Malaria Journal*, 11(1):271, 2012.

[31] M. Pascual, B. Cazelles, M. Bouma, L. Chaves, and K. Koelle. Shifting patterns: malaria dynamics and rainfall variability in an african highland. *Proceedings of the Royal Society B: Biological Sciences*, 275(1631):123–132, 2007.

[32] M. Sewe, J. Rocklöv, J. Williamson, M. Hamel, A. Nyaguara, F. Odhiambo, and K. Laserson. The association of weather variability and under five malaria mortality in kemri/cdc hdss in western kenya 2003 to 2008: a time series analysis. *International journal of environmental research and public health*, 12(2):1983–1997, 2015.

[33] J. Shaman and J. F. Day. Reproductive phase locking of mosquito populations in response to rainfall frequency. *PLoS One*, 2(3):e331, 2007.

[34] A. S. Siraj, M. Santos-Vega, M. Bouma, D. Yadeta, D. R. Carrascal, and M. A. C. Pascual. Altitudinal changes in malaria incidence in highlands of ethiopia and colombia. *Science*, 343:1154–1158, 2014.

[35] P. Van den Driessche and J. Watmough. Reproduction numbers and sub-threshold endemic equilibria for compartmental models of disease transmission. *Mathematical biosciences*, 180(1-2):29–48, 2002.

[36] L. Wang, Z. Teng, and T. Zhang. Threshold dynamics of a malaria transmission model in periodic environment. *Communications in Nonlinear Science and Numerical Simulation*, 18(5):1288–1303, 2013.

[37] W. Wang and X.-Q. Zhao. Threshold dynamics for compartmental epidemic models in periodic environments. *Journal of Dynamics and Differential Equations*, 20(3):699–717, 2008.

[38] Y. Yang and Y. Xiao. Threshold dynamics for an hiv model in periodic environments. *Journal of Mathematical Analysis and Applications*, 361(1):59–68, 2010.